

Spontaneous emission of a chiral molecule near a cluster of two chiral spherical particles

D.V. Guzatov, V.V. Klimov

Abstract. We have obtained and investigated analytical expressions for the radiative spontaneous decay rate of a chiral (optically active) molecule located near a cluster of two identical chiral (bi-isotropic) spherical particles. It is found that the composition of the particles, their location and size have a significant effect on the spontaneous emission of chiral molecules. In particular, it is shown that in the case of nanoparticles of chiral metamaterials, the radiative spontaneous decay rate for the ‘right-’ and ‘left-handed’ enantiomers of chiral molecules located in the gap of the cluster are significantly different.

Keywords: spontaneous emission, chiral molecule, enantiomer, two-particle cluster, metamaterial.

Introduction

Chirality is a geometric property of three-dimensional bodies to be asymmetric with their mirror image in the case of any translation and rotation. Human hands and springs are universally recognised examples of this property. Chirality plays an important role in biology and pharmaceuticals, because many complex organic compounds (amino acids, proteins) have chiral properties. For this reason, the body can completely differently react to various isomers of the same substance. For example, the same drug, depending on which type of molecules it consists, can have different taste and smell or have different effects. In physics, of considerable interest are chiral media [1], in which one can observe a difference between the propagation of left- and right-hand circularly polarised electromagnetic waves, which leads to a number of interesting optical phenomena, such as the rotation of the polarisation plane, circular dichroism and others. At present, the study of chiral properties is again in the spotlight because of the ability to produce metamaterials based on chiral meta-atoms [2–5].

Spontaneous emission of atoms and molecules located near material bodies has been studied in many papers. The effect of dielectric microspheres on spontaneous emission of atoms was considered in [6–8]; spontaneous decay of an atom

located near a microsphere of a negative-index metamaterial was investigated in [9]; spontaneous emission of atoms and molecules near a cluster of two spherical nanoparticles was studied in [10–12]. At the same time, only recently researchers turned their attention to the effect of chiral particles on the emission of chiral molecules. In particular, we considered in [13–15] the influence of a spherical nanoparticle on the emission of a chiral molecule. At the same time, a cluster of two nanoparticles has more interesting properties. In fact, such a cluster is a chiral nanoantenna, which can be used to effectively control both field emission and detection.

To our knowledge, the emission of chiral molecules near a cluster of chiral spherical particles has not yet been considered in the literature, and so the purpose of this paper is a theoretical study of the effect of a cluster of two identical chiral (bi-isotropic) spherical particles on the spontaneous emission of a chiral (optically active) molecule. All analytical results will be obtained for arbitrary sizes of particles and distances between them, an arbitrary composition of the particle substances and an arbitrary relation between the electric and magnetic dipole moments of the chiral molecule.

The paper has the following structure. In Section 2 we consider the electromagnetic field in the presence of a cluster of two chiral spherical particles. At the same time, despite the fact that the chirality can be regarded as a manifestation of spatial dispersion, we use conventional (local) boundary conditions at the interface between the two media. A more general approach using nonlocal boundary conditions was developed in [16, 17]. In Section 3 we derive general expressions for the radiative spontaneous decay rate of a chiral molecule located near the cluster. In Section 4 we provide a graphic illustration of the results and their discussion, and in Section 5 (Conclusions) the main results are presented.

Electromagnetic field of a chiral molecule in the presence of a cluster of two chiral spherical particles

In describing the electric and magnetic fields in a chiral environment, we will use the Drude–Born–Fedorov constitutive equations [18–20]:

$$\mathbf{D} = \varepsilon(\mathbf{E} + \eta \text{rot} \mathbf{E}), \quad \mathbf{B} = \mu(\mathbf{H} + \eta \text{rot} \mathbf{H}), \quad (1)$$

where \mathbf{D} , \mathbf{E} and \mathbf{B} , \mathbf{H} are the electric and magnetic field induction and strength, respectively; ε and μ are the permittivity and permeability of the chiral material; η is the dimensional parameter of chirality; and the time dependence of the fields

D.V. Guzatov Yanka Kupala State University of Grodno, ul. Ozheshko 22, 230023 Grodno, Belarus; e-mail: dm_guzatov@mail.ru;

V.V. Klimov P.N. Lebedev Physics Institute, Russian Academy of Sciences, Leninsky prosp. 53, 119991 Moscow, Russia; National Research Nuclear University ‘MEPhI’, Kashirskoe shosse 31, 115409 Moscow, Russia; e-mail: vklim@sci.lebedev.ru

Received 21 January 2014; revision received 11 June 2014

Kvantovaya Elektronika 45 (3) 250–257 (2015)

Translated by I.A. Ulitkin

is determined by the factor $\exp(-i\omega t)$, which is hereinafter omitted.

Selection of constitutive equations in form (1) is somewhat arbitrary. Another possibility is to use, for example, constitutive equations in the Boys–Post representation:

$$\mathbf{D} = \varepsilon \mathbf{E} + i \frac{\kappa}{c} \mathbf{B}, \quad \mathbf{H} = \frac{1}{\mu} \mathbf{B} + i \frac{\kappa}{c} \mathbf{E}, \quad (2)$$

where κ is the chirality parameter and c is the speed of light. There are even some indications that the constitutive equations in form of (2) are more fundamental than in form (1) [21]. The debate about the choice of constitutive equations is presented, for example, in monograph [22]. The particular form of constitutive equations leads to some boundary conditions, which, in the case of chiral media, do not fortunately prevent the solution of the problem by the method of separation of variables. Therefore, for definiteness, we consider relations (1) for which the boundary conditions are reduced to the continuity of the tangential components of the electric and magnetic fields.

To solve the problem of the emission of a molecule near a cluster of two chiral spherical particles, we will use the standard T-matrix method. This method is often used to describe clusters of spherical particles. In principle, this method is accurate and based on Mie theory for each particle and the addition theorem for vector spherical harmonics [23–31]. Initially, the method was developed by Waterman [32] and further significantly improved in [33–37]. The procedure for the analytical calculation of the T-matrix for a cluster of spheres is thoroughly described in [28]. A detailed bibliography on this method can be found in monograph [38].

In the case of a cluster of two chiral spherical particles, the T-matrix method makes use of two local coordinate systems associated with each cluster particle. For definiteness, we assume that the local Cartesian coordinate systems have parallel and equally directed axes and a common axis z , while their origins are located in the centres of spherical particles (Fig. 1). The coordinates and all other values related to the s th ($s = 1, 2$) particle will be denoted by an additional index 1 or 2. Below, we will consider a cluster of two identical spherical particles with radii a , made of the chiral material with permittivity ε and permeability μ , as well as the dimensionless chirality parameter χ . Let the cluster be located in an environment with unit values of permittivity and permeability. The case of a cluster of two different chiral spherical particles can be considered similarly.

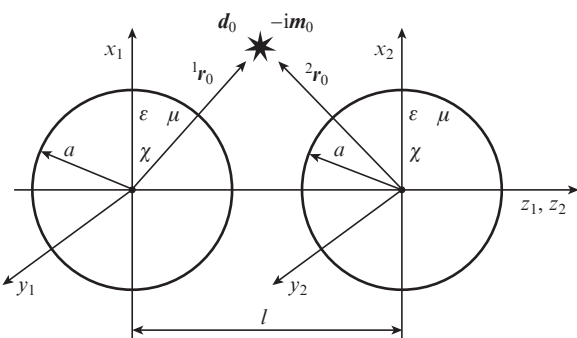


Figure 1. Geometry of the problem of a chiral molecule located near a cluster of two chiral spherical particles.

As usual, to solve the problem of the emission of the molecule near a cluster we need to write out arbitrary expressions for the fields outside of particles with allowance for the emitting molecule and arbitrary expressions for the fields inside the particles. Then, using the boundary conditions on the surface of the particles we find the unknown coefficients of the expansion.

We first write out the expression for the fields outside of particles. The electric and magnetic field strengths of the chiral molecule with the electric and magnetic dipole moments \mathbf{d}_0 and $-i\mathbf{m}_0$, respectively, are defined in the free space by the electric and magnetic Hertz vectors, and in the local coordinate system associated with the centre of the s th particle, the expression for them have the form

$$\begin{aligned} {}^s\mathbf{E}_0 &= \{(\mathbf{d}_0 \nabla) \nabla + \mathbf{d}_0 k_0^2 - ik_0 [(-i\mathbf{m}_0), \nabla]\} \\ &\times \frac{\exp(ik_0 |{}^s\mathbf{r} - {}^s\mathbf{r}_0|)}{|{}^s\mathbf{r} - {}^s\mathbf{r}_0|}, \quad {}^s\mathbf{H}_0 = \frac{1}{ik_0} \text{rot } {}^s\mathbf{E}_0, \end{aligned} \quad (3)$$

where ∇ is the gradient operator; ${}^s\mathbf{r}$ and ${}^s\mathbf{r}_0$ are the radius vectors of the observation points and chiral molecule locations, respectively; and $k_0 = \omega/c$ is the wavenumber in vacuum. The above-used phase relationship between the electric \mathbf{d}_0 and magnetic $-i\mathbf{m}_0$ dipole moments is caused by the choice of the chiral molecules in the form of a spiral. Note that the Cartesian components of the vectors \mathbf{d}_0 and $-i\mathbf{m}_0$, as well as the Cartesian components of the gradient operators and rotor will not change in passing from one local coordinate system to another, because the axes of the local systems are parallel and equally directed.

Using the representation of the electric dipole field in spherical coordinates [39], for the electric field strength of the chiral molecule (3) in local spherical coordinates associated with the s th particle, we find the expressions:

$${}^s\mathbf{E}_0 = \begin{cases} \sum_{n=1}^{\infty} \sum_{m=-n}^n [{}^sA_{mn}^{(0)} {}^s\mathcal{N}\psi_{mn}^{(0)} + {}^sB_{mn}^{(0)} {}^s\mathcal{M}\psi_{mn}^{(0)}], & |{}^s\mathbf{r}| < |{}^s\mathbf{r}_0|, \\ \sum_{n=1}^{\infty} \sum_{m=-n}^n [{}^sC_{mn}^{(0)} {}^s\mathcal{N}\zeta_{mn} + {}^sD_{mn}^{(0)} {}^s\mathcal{M}\zeta_{mn}], & |{}^s\mathbf{r}| > |{}^s\mathbf{r}_0|, \end{cases} \quad (4)$$

where ${}^s\mathcal{N}\psi_{mn}^{(0)}$, ${}^s\mathcal{M}\psi_{mn}^{(0)}$, ${}^s\mathcal{N}\zeta_{mn}$ and ${}^s\mathcal{M}\zeta_{mn}$ are the vector spherical harmonics [14, 29], and the coefficients ${}^sA_{mn}^{(0)}$, ${}^sB_{mn}^{(0)}$, ${}^sC_{mn}^{(0)}$ and ${}^sD_{mn}^{(0)}$ are given in the Appendix. The magnetic field strength of the molecule can be found from expression (3).

Scattered electric and magnetic fields induced outside of the clusters can be represented as the sum of the partial fields from each particle, expressed in local coordinates [29]:

$$\mathbf{E}^{\text{out}} = \sum_{s=1}^2 {}^s\mathbf{E}^{\text{out}}, \quad \mathbf{H}^{\text{out}} = \sum_{s=1}^2 {}^s\mathbf{H}^{\text{out}}, \quad (5)$$

where

$$\begin{aligned} {}^s\mathbf{E}^{\text{out}} &= \sum_{n=1}^{\infty} \sum_{m=-n}^n ({}^sC_{mn} {}^s\mathcal{N}\zeta_{mn} + {}^sD_{mn} {}^s\mathcal{M}\zeta_{mn}); \\ {}^s\mathbf{H}^{\text{out}} &= \frac{1}{ik_0} \text{rot } {}^s\mathbf{E}^{\text{out}}, \end{aligned} \quad (6)$$

and the coefficients ${}^sC_{mn}$ and ${}^sD_{mn}$ should be found by means of boundary conditions. The total field outside of the particles is thus determined by the sum of expressions (4) and (5).

To describe the electromagnetic fields inside each particle, after using the Bohren transform [40], solution to (1) can be written as

$$\begin{pmatrix} \mathbf{E} \\ \mathbf{H} \end{pmatrix} = \hat{A} \begin{pmatrix} \mathbf{Q}_L \\ \mathbf{Q}_R \end{pmatrix}, \quad \hat{A} = \begin{pmatrix} 1 & -iZ \\ -i/Z & 1 \end{pmatrix}, \quad (7)$$

where $Z = \mu/\sqrt{\varepsilon\mu}$, and the components of the transformed field satisfy the equations [40]

$$\begin{aligned} \text{rot} \mathbf{Q}_L &= +k_L \mathbf{Q}_L, \quad \text{div} \mathbf{Q}_L = 0, \\ \text{rot} \mathbf{Q}_R &= -k_R \mathbf{Q}_R, \quad \text{div} \mathbf{Q}_R = 0, \end{aligned} \quad (8)$$

where

$$k_L = \frac{k_0 \sqrt{\varepsilon\mu}}{1 - \chi \sqrt{\varepsilon\mu}}, \quad k_R = \frac{k_0 \sqrt{\varepsilon\mu}}{1 + \chi \sqrt{\varepsilon\mu}} \quad (9)$$

are the wavenumbers of waves with left- (L) and right-hand (R) circular polarisations; and $\chi = k_0 \eta$ is the dimensionless chirality parameter, which is considered small: $|\chi \sqrt{\varepsilon\mu}| < 1$. The opposite case, $|\chi \sqrt{\varepsilon\mu}| > 1$, corresponds to a different physics and will be discussed in a separate publication. Note that in this paper we take $\sqrt{\varepsilon\mu} = \sqrt{\varepsilon} \sqrt{\mu}$. Such a definition of square roots provides the correct refractive indices of materials of various types, as well as the positive coefficients of extinction.

The expressions for the electric and magnetic field strengths inside the s th chiral particle, according to (7), have the form

$${}^s \mathbf{E}^{\text{in}} = {}^s \mathbf{Q}_L - iZ {}^s \mathbf{Q}_R, \quad {}^s \mathbf{H}^{\text{in}} = -\frac{i}{Z} {}^s \mathbf{Q}_L + {}^s \mathbf{Q}_R, \quad (10)$$

where

$${}^s \mathbf{Q}_L = \sum_{n=1}^{\infty} \sum_{m=-n}^n {}^s A_{nm} ({}^s \mathbf{N}\psi_{mn}^L + {}^s \mathbf{M}\psi_{mn}^L); \quad (11)$$

$${}^s \mathbf{Q}_R = \sum_{n=1}^{\infty} \sum_{m=-n}^n {}^s B_{nm} ({}^s \mathbf{N}\psi_{mn}^R - {}^s \mathbf{M}\psi_{mn}^R);$$

${}^s \mathbf{N}\psi_{mn}^{(J)}$ and ${}^s \mathbf{M}\psi_{mn}^{(J)}$ ($J = L, R$) are the vector spherical harmonics [14]; and expansion coefficients ${}^s A_{nm}$ and ${}^s B_{nm}$ can be found by means of boundary conditions. It follows from (11) that ${}^s \mathbf{Q}_L$ and ${}^s \mathbf{Q}_R$ are expressed in terms of a fixed combination of vector harmonics ${}^s \mathbf{N}\psi_{mn}^L + {}^s \mathbf{M}\psi_{mn}^L$ and ${}^s \mathbf{N}\psi_{mn}^R - {}^s \mathbf{M}\psi_{mn}^R$, which always have a nonzero component along the radius and, therefore, cannot be reduced to the ordinary TM or TE fields.

To find the unknown coefficients of expansions (11) and (6) we will use the boundary conditions of continuity of the tangential components of the electric and magnetic field strengths on the surface of spheres [41], as well as the theorem of addition of vector spherical harmonics [29–31]. This theorem allows the vector harmonic describing the fields outside of the cluster in some local coordinates (for example, for $s = 2$) to be represented in the form of expansions in harmonics written in other local coordinates ($s = 1$), as is pointed out in the Appendix. Substituting these expansions into (6), we obtain expressions for the strengths ${}^2 \mathbf{E}^{\text{out}}$ and ${}^2 \mathbf{H}^{\text{out}}$ ($s = 2$) in

the form of series over the vector spherical harmonics in the coordinates of the first sphere ($s = 1$). The thus-found expressions are added to the expressions for ${}^1 \mathbf{E}^{\text{out}}$ and ${}^1 \mathbf{H}^{\text{out}}$ ($s = 1$) [see Eqn (5)] and can already be used to sew the fields on the surface of the first particle. Analogous steps are carried out by using the boundary conditions on the surface of the second particle.

Because the molecule in question is located outside of the spherical particles, then to find the spontaneous decay rate, which is expressed in terms of the energy flux at infinity, we will not need the relations for the coefficients ${}^1 A_{nm}$, ${}^1 B_{nm}$, ${}^2 A_{nm}$ and ${}^2 B_{nm}$ included in the formula for the fields inside the spheres. For the coefficients ${}^1 C_{mn}$, ${}^1 D_{mn}$, ${}^2 C_{mn}$ and ${}^2 D_{mn}$, which describe the scattered field, we can obtain the systems of equations:

$$\begin{aligned} {}^1 C_{mn} + \sum_{q=|m|}^{\infty} (V_{mnq} \alpha_n - i W_{mnq} \delta_n) {}^2 C_{mq} \\ + \sum_{q=|m|}^{\infty} (W_{mnq} \alpha_n - i V_{mnq} \delta_n) {}^2 D_{mq} = -\alpha_n {}^1 A_{mn}^{(0)} + i \delta_n {}^1 B_{mn}^{(0)}, \end{aligned} \quad (12)$$

$$\begin{aligned} {}^1 D_{mn} + \sum_{q=|m|}^{\infty} (V_{mnq} \beta_n - i W_{mnq} \delta_n) {}^2 D_{mq} \\ + \sum_{q=|m|}^{\infty} (W_{mnq} \beta_n - i V_{mnq} \delta_n) {}^2 C_{mq} = -\beta_n {}^1 B_{mn}^{(0)} + i \delta_n {}^1 A_{mn}^{(0)}, \end{aligned}$$

$$\begin{aligned} {}^2 C_{mn} + \sum_{q=|m|}^{\infty} (-1)^{q+n} (V_{mnq} \alpha_n + i W_{mnq} \delta_n) {}^1 C_{mq} \\ - \sum_{q=|m|}^{\infty} (-1)^{q+n} (W_{mnq} \alpha_n + i V_{mnq} \delta_n) {}^1 D_{mq} = -\alpha_n {}^2 A_{mn}^{(0)} + i \delta_n {}^2 B_{mn}^{(0)}, \end{aligned} \quad (13)$$

$$\begin{aligned} {}^2 D_{mn} + \sum_{q=|m|}^{\infty} (-1)^{q+n} (V_{mnq} \beta_n + i W_{mnq} \delta_n) {}^1 D_{mq} \\ - \sum_{q=|m|}^{\infty} (-1)^{q+n} (W_{mnq} \beta_n + i V_{mnq} \delta_n) {}^1 C_{mq} = -\beta_n {}^2 B_{mn}^{(0)} + i \delta_n {}^2 A_{mn}^{(0)}, \end{aligned}$$

where the lower limit of the summation over q should be assumed equal to 1 for $m = 0$ and equal to $|m|$ for $m \neq 0$; and the functions V_{mnq} and W_{mnq} are given in the Appendix. The expressions for the scattering coefficients α_n , β_n and δ_n have the form

$$\begin{aligned} \alpha_n = \frac{A_n^L W_n^R + A_n^R W_n^L}{V_n^L W_n^R + V_n^R W_n^L}, \quad \beta_n = \frac{V_n^L B_n^R + V_n^R B_n^L}{V_n^L W_n^R + V_n^R W_n^L}, \\ \delta_n = -i \frac{V_n^L A_n^R - V_n^R A_n^L}{V_n^L W_n^R + V_n^R W_n^L} = i \frac{B_n^L W_n^R - B_n^R W_n^L}{V_n^L W_n^R + V_n^R W_n^L}, \end{aligned} \quad (14)$$

where we have introduced the notation ($J = L, R$)

$$\begin{aligned} A_n^{(J)} &= \psi_n(k_J a) \psi'_n(k_0 a) - Z \psi'_n(k_J a) \psi_n(k_0 a); \\ B_n^{(J)} &= Z \psi_n(k_J a) \psi'_n(k_0 a) - \psi'_n(k_J a) \psi_n(k_0 a); \\ V_n^{(J)} &= \psi_n(k_J a) \zeta'_n(k_0 a) - Z \psi'_n(k_J a) \zeta_n(k_0 a); \\ W_n^{(J)} &= Z \psi_n(k_J a) \zeta'_n(k_0 a) - \psi'_n(k_J a) \zeta_n(k_0 a); \end{aligned} \quad (15)$$

the Riccati–Bessel functions $\psi_n(k_J a)$ and $\zeta_n(k_0 a)$ are defined in the Appendix; and the prime at the function denotes the derivative with respect to its argument.

As seen from (12) and (13), the structure of the equations obtained is that the subscript n changes in them, while the subscript m can be fixed. In the numerical solution of (12) and (13) use is made of the truncated equations with $n \leq N_{\max}$. In this case, the greater the N_{\max} , the more accurate the results for the coefficients ${}^s C_{mm}$ and ${}^s D_{mm}$, which is due to their tendency to zero at $n \rightarrow \infty$ [42]. The relative positioning of the spherical particles should also be taken into account: the closer they are to each other, the greater N_{\max} one must use to achieve a predetermined accuracy [42].

Radiative spontaneous decay rate of a chiral molecule near a cluster of two chiral spherical particles

The relative radiative spontaneous decay rate of a chiral molecule near a cluster of two chiral spherical particles can be calculated as the ratio of the total emission power P_{rad} of a molecule + cluster system to the emission power $P_{\text{rad}0}$ of the molecules in the absence of a cluster [43]. The power P_{rad} is calculated by the formula [41]

$$P_{\text{rad}} = \frac{c}{8\pi} \int_S dS \operatorname{Re} \{ [(\mathbf{E}^{\text{out}} + {}^s \mathbf{E}_0), (\mathbf{H}^{\text{out}*} + {}^s \mathbf{H}_0^*)] \cdot \mathbf{n} \}, \quad (16)$$

where integration is performed over a closed surface S , covering the molecule and particles; \mathbf{n} is the outward normal to this surface. The power $P_{\text{rad}0}$ can easily be found from (16) if we put the scattered field equal to zero:

$$P_{\text{rad}0} = \frac{ck_0^4}{3} (|\mathbf{d}_0|^2 + |\mathbf{m}_0|^2). \quad (17)$$

Of course, this expression coincides with the total radiation power of the electric and magnetic dipoles, because they exhibit no interference with each other.

As the surface S , over which the integration in (16) is performed, it is convenient to take a sphere of infinite radius with its centre coinciding with the centre of any of the local coordinate systems. For example, by performing calculations in the local coordinates associated with the first particle ($s = 1$), and normalising to the radiation power in free space, we find for the radiative rate γ_{rad} the expression

$$\frac{\gamma_{\text{rad}}}{\gamma_0} = \frac{P_{\text{rad}}}{P_{\text{rad}0}} = \frac{3}{2k_0^6 (|\mathbf{d}_0|^2 + |\mathbf{m}_0|^2)} \times \sum_{n=1}^{\infty} \sum_{m=-n}^n \frac{n(n+1)}{2n+1} \frac{(n+m)!}{(n-m)!} (|{}^1 C_{mm}^{(0)} + \tilde{C}_{mm}|^2 + |{}^1 D_{mm}^{(0)} + \tilde{D}_{mm}|^2), \quad (18)$$

where $\gamma_0 = P_{\text{rad}0}/(h\nu)$ is the spontaneous decay rate of a chiral molecule in free space; and

$$\tilde{C}_{mm} = {}^1 C_{mm} + \sum_{q=|m|}^{\infty} (\tilde{V}_{mnq} {}^2 C_{mq} + \tilde{W}_{mnq} {}^2 D_{mq}), \quad (19)$$

$$\tilde{D}_{mm} = {}^1 D_{mm} + \sum_{q=|m|}^{\infty} (\tilde{V}_{mnq} {}^2 D_{mq} + \tilde{W}_{mnq} {}^2 C_{mq}).$$

In expressions (19), the lower limit of summation over q should be assumed equal to 1 for $m = 0$ and equal to $|m|$ for

$m \neq 0$; the functions \tilde{V}_{mnq} and \tilde{W}_{mnq} are given in the Appendix. It should be noted that relation (18) corresponds to the transition of a molecule from some excited state to the ground state, i.e., to the case of a two-level molecule. In this case, \mathbf{d}_0 and $-\mathbf{im}_0$ should be regarded as the electric and magnetic dipole moments of the transition. To account for the possibility of transition to some states it is only necessary to sum the corresponding partial widths of the lines (18).

Analysis of the results and graphic illustrations

The process of spontaneous emission of a chiral molecule located near a cluster of two chiral spherical particles is very complex, and below for clarity we will present graphic illustrations of some possible regimes of interaction of a chiral molecule with clusters of various compositions. Here we restrict our consideration to the most interesting case, when the chiral molecule is in the gap between chiral particles on the common axis z , passing through the centres of the particles (Fig. 1), because in this case, the local fields are maximal. In this geometry, the position of the molecule is described by the angles ${}^1\theta_0 = 0$ and ${}^2\theta_0 = \pi$, and the expressions for the coefficients ${}^s A_{mm}^{(0)}$, ${}^s B_{mm}^{(0)}$, ${}^s C_{mm}^{(0)}$ and ${}^s D_{mm}^{(0)}$ are greatly simplified (see the Appendix); therefore, nonzero are only the coefficients ${}^s C_{mm}$ and ${}^s D_{mm}$ with $m = 0, \pm 1$.

Below, we consider a chiral molecule with equal Cartesian projections of the electric ($d_{0x} = d_{0y} = d_{0z}$) and magnetic ($m_{0x} = m_{0y} = m_{0z}$) dipole moments. This choice of the molecule allows one to study all the features of spontaneous emission at the same time, because modes of all types are excited in the spheres. In this case, we call the molecule with parallel \mathbf{m}_0 and \mathbf{d}_0 the right-handed molecules, and molecules with antiparallel \mathbf{m}_0 and \mathbf{d}_0 – the left-handed molecules.

Figure 2 shows the dependences of the radiative spontaneous decay rate of a chiral molecule located in the gap of a cluster of two dielectric particles near the surface of the first particle on the particle size $k_0 a$, for the case of particles with no chiral properties (Fig. 2a) and a small chirality (Fig. 2b) at different relative distances $l/(2a)$ between the particles. One can clearly see that at large distances between the particles, the spontaneous decay rate tends to the decay rate for a single particle. This is not done in the case of close proximity of the particles. Very important here is that the maximum radiative spontaneous decay rate occurs for the spheres of small size (or longer wavelengths).

Chirality of spherical particles leads to a redistribution of the positions of the maximum radiative spontaneous decay rate and to the emergence of high- Q , as compared with the case of a cluster of non-chiral particle, resonances (cf. Figs 2a and b). In general, the presence of chirality increases the spontaneous decay rate. It is very important is that, compared with non-chiral spheres, there is a noticeable difference between the radiative spontaneous decay rates for the right- and left-handed molecules (Fig. 2b).

Figure 3 shows the spontaneous decay rate of a chiral molecule located near a chiral spherical particle (Fig. 3a) and in the gap between two chiral particles near the surface of the first of them (Fig. 3b) as a function of the chirality parameter χ . One can clearly see that the dependence of the radiative spontaneous decay rate of a molecule in the gap of a cluster on the chirality parameter changes significantly as compared with the case of a molecule near a single sphere. The most significant differences arise for chiral particles made of a negative-index

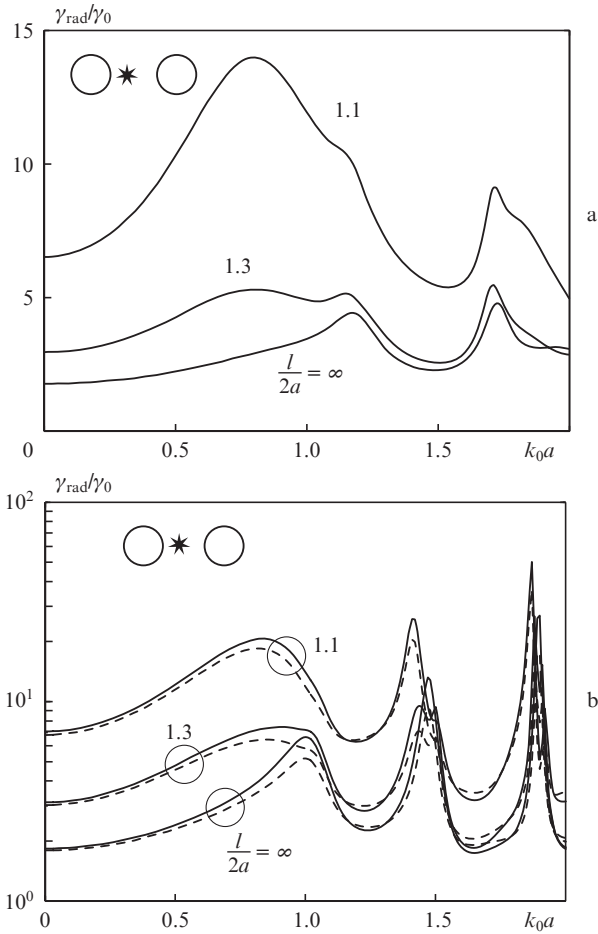


Figure 2. Radiative spontaneous decay rate of a chiral molecule located near the surface of the first spherical cluster particle (${}^1r_0 \rightarrow a, {}^2r_0 = l - a$) as a function of the particle size k_0a at different relative distances between the particles $l/(2a)$. Permittivity and permeability of the particles are $\epsilon = 6$ and $\mu = 1$, the chirality parameter is $\chi = (a)$ 0 and (b) 0.1. The case of a single particle [$l/(2a) = \infty$] corresponds to the position of the molecule near the surface of the particles on the positive part of the z axis. Solid curves correspond to the right-handed molecule ($\mathbf{m}_0 = +0.1\mathbf{d}_0$), and dashed curves – to the left-handed molecule ($\mathbf{m}_0 = -0.1\mathbf{d}_0$). In the case of non-chiral particles the dependences for the right- and left-handed molecules coincide.

metamaterial ($\epsilon = -4, \mu = -1.1$). One can also see that at a close proximity of such particles [$l/(2a) = 1.1$] there appears a large number of high- Q maxima in the dependence of the radiative rate on χ , and the dependence itself becomes much more complicated than for a single particle. Apparently, this is due to the fact that in a cluster of two chiral spherical negative-index particles, modes highly localised in the gap, which are absent in the case of a single particle, are excited. These modes occur in the case of a cluster of two metal nanoparticles [11].

The case of a cluster of two chiral spherical particles with the properties of a dielectric ($\epsilon = 4, \mu = 1$) also differs from that of a single chiral dielectric sphere. In particular, it is clearly seen that the number of radiative spontaneous decay rate maxima increases, but not as much as for the particles of the metamaterial.

For chiral particles having metal properties ($\epsilon = -4, \mu = 1$), the dependence of the radiative spontaneous decay rate on χ is weakly expressed, which is due to an imaginary refractive index $\sqrt{\epsilon\mu}$, i.e., the absence of the waves propagating in the spheres. Noticeable only is an increase in the radiative spon-

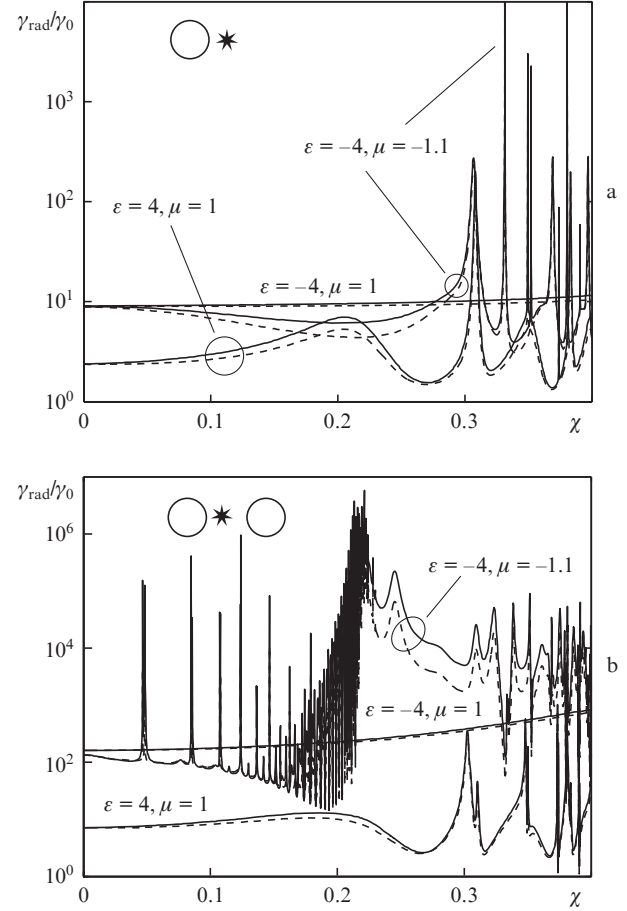


Figure 3. Dependences of the radiative spontaneous decay rate of a chiral molecule on the chirality parameter χ . The molecule is located (a) near the surface of a single spherical particle on the positive part of the z axis (${}^1r_0 \rightarrow a, {}^2r_0 \rightarrow \infty$) and (b) near the surface of the first spherical cluster particle (${}^1r_0 \rightarrow a, {}^2r_0 = l - a$). Solid curves correspond to the right-handed molecule ($\mathbf{m}_0 = +0.1\mathbf{d}_0$), and dashed curves – to the left-handed molecule ($\mathbf{m}_0 = -0.1\mathbf{d}_0$). The relative distance between the cluster particles is $l/(2a) = 1.1$, and the particle size is $k_0a = 1$.

aneous decay rate for a molecule in the cluster gap as compared with a molecule near a single particle (cf. Figs 3a and b).

Note here that for a significant difference between the spontaneous decay rates to be observed for the right- and left-handed molecules, a sufficiently large value of chirality is needed. Currently, for chiral metamaterials it is possible in the radio range [44, 45]. Nevertheless, reducing the size of chiral meta-atoms [46] allows us to hope to obtain similar results in the microwave and optical ranges.

Figure 4 shows the radiative spontaneous decay rate of a chiral molecule located near a single chiral spherical nanoparticle (Fig. 4a) and in the gap between the cluster nanoparticles near the surface of the first nanosphere (Fig. 4b) as a function of permittivity for a given permeability ($\mu = -1.6$). One can see that for the right- and left-handed enantiomers of the molecules the radiative spontaneous decay rate takes significantly different values and, therefore, may effectively control their properties [13]. In the case of a cluster of nanoparticles, one can observe an increase, compared with the case of a single nanoparticle, in the number of radiative spontaneous decay rate maxima, which is due to a large number of excited surface (chiral plasmon) modes in the cluster. An increase in the number of excited modes allows one to control the spontane-

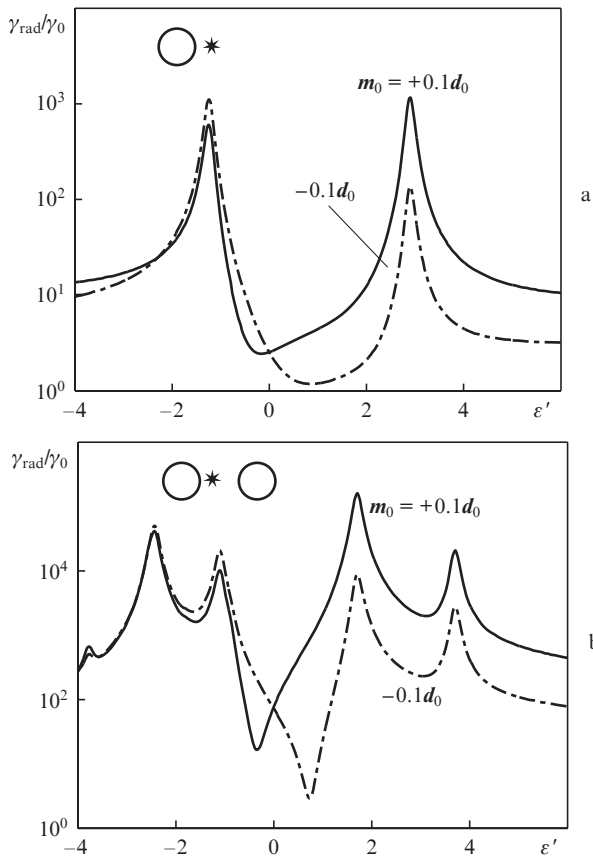


Figure 4. Dependences of the radiative spontaneous decay rate of the right- ($m_0 = +0.1d_0$) and left-handed ($m_0 = -0.1d_0$) chiral molecules on the real part of permittivity $\epsilon = \epsilon' + i0.1$ at $\mu = -1.6$, $k_0a = 0.1$ и $\chi = 0.2$. The molecule is located (a) near the surface of a single spherical particle on the positive part of the z axis (${}^1r \rightarrow a$, ${}^2r \rightarrow \infty$) and (b) near the surface of the first spherical cluster particle (${}^1r_0 \rightarrow a$, ${}^2r_0 = l - a$). The relative distance between the particles is $l/(2a) = 1.1$.

ous emission of a chiral molecule located in the gap of the cluster by changing the distance between nanoparticles. Furthermore, a comparison of Figs 4a and b shows that the radiative spontaneous decay rate for a chiral molecule in the gap between nanospheres takes significantly larger values than for the molecules near a single nanoparticle.

Chiral molecules play a particularly important role in biology and pharmacy. It is therefore extremely important to be able to carry out the selection of the right- and left-handed enantiomers of chiral molecules in racemic mixtures. Figure 5 shows the ratio of the spontaneous emission rate for the left-handed molecule to the decay rate for the right-handed molecule ($\gamma_{\text{rad}}^L/\gamma_{\text{rad}}^R$) and an inverse ratio ($\gamma_{\text{rad}}^R/\gamma_{\text{rad}}^L$) as a function of the permittivity and permeability of the cluster of two chiral spherical nanoparticles. The molecule is located in the gap between nanoparticles near the surface of the first nanoparticle. One can see that at certain values of ϵ and μ there is a significant difference in the radiative spontaneous decay rates for the right- and left-handed enantiomers of molecules: by about 40 or even about 300 (or more) times, depending on the molecule chirality which should be regarded as a reference one. In the case of similar single chiral nanospheres the difference in radiative spontaneous decay rates of enantiomers is also very significant: by about 15 and 60 times [13].

A significant difference between the emission rates of right- and left-handed molecules located in the gap of the cluster of

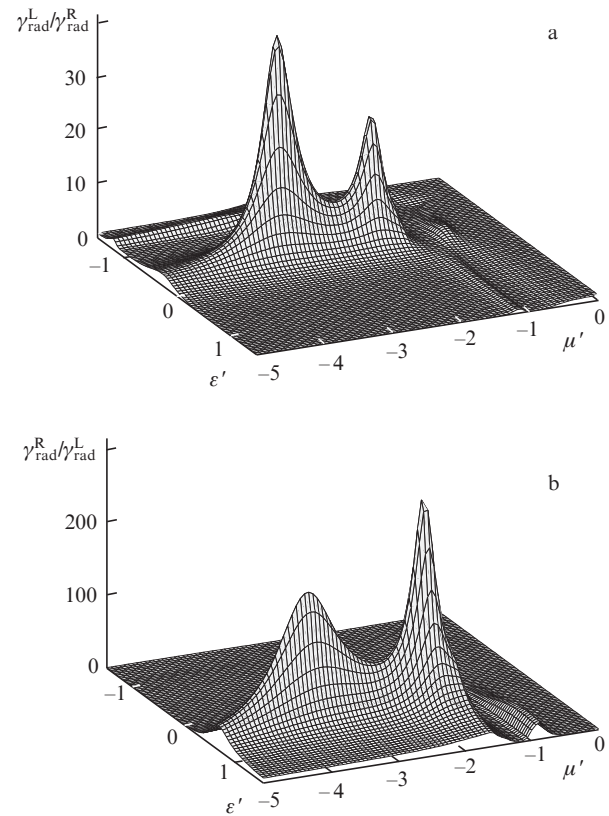


Figure 5. (a) Ratio of the radiative spontaneous decay rate of the left-handed ($m_0 = -0.1d_0$) chiral molecule to the radiative spontaneous decay rate of the right-handed ($m_0 = +0.1d_0$) chiral molecule and (b) inverse ratio as functions of the real parts of permittivity ($\epsilon = \epsilon' + i0.1$) and permeability ($\mu = \mu' + i0.1$) of the material of which is made a cluster of two spherical chiral particles with $k_0a = 0.1$ and $\chi = 0.2$. The molecule is located near the surface of the first spherical cluster particle (${}^1r_0 \rightarrow a$, ${}^2r_0 = l - a$). The relative distance between the particles is $l/(2a) = 1.1$.

two chiral metamaterial nanoparticles can form the basis for designing devices that allow for the detection and selection of enantiomers of chiral molecules in racemic mixtures in a similar way as it can be done in the case of single nanoparticles [13]. One can see from Fig. 5 that a cluster of nanoparticles with simultaneously negative ϵ and μ will accelerate the decay of the left-handed molecules and slow it down for the right-handed molecules, and a cluster of nanoparticles with $\epsilon > 0$ and $\mu < 0$ will, on the contrary, accelerate the decay for the right-handed molecules and slow it down for the left-handed molecules. At the same time, from a practical point of view, the most suitable are chiral metamaterial particles with $\epsilon > 0$ and $\mu < 0$, because the technology of their production (technology of split ring resonators) is currently well developed [47, 48].

Conclusions

Thus, we have derived analytical expressions for the radiative spontaneous decay rate of a chiral (optically active) molecule located near a cluster of two identical chiral (bi-isotropic) spherical particles with an arbitrary material composition, size and mutual arrangement. We have studied the features of the spontaneous emission of the right- and left-handed enantiomers of chiral molecules for chiral clusters of different materials.

It is shown that for chiral molecules in the gap between chiral metamaterial cluster nanoparticles with simultaneously

negative permittivity and permeability, as well as chiral material nanoparticles with negative magnetic permeability and positive permittivity, the right- and left-handed enantiomers of molecules exhibit a significant difference between the radiative spontaneous decay rates which may be markedly larger than in the case of single chiral nanoparticles.

The results obtained can be used to calculate the radiative spontaneous decay rate for chiral molecules located near a cluster of two chiral spherical particles, for the interpretation of experimental data on the interaction of chiral molecules and chiral particles and for the design of nanobiosensors.

In this paper, we have considered only the radiative spontaneous decay rate (the rate of spontaneous emission), because this quantity is measured by a detector. A nonradiative channel of spontaneous decay, i.e., the channel associated with the Joule losses in the sphere material, will be discussed in a separate publication.

Acknowledgements. The authors express their gratitude to the Belarusian Republican Foundation for Fundamental Research (Grant No. F12R-006), Russian Foundation for Basic Research (Grant Nos 14-02-00290 and 15-52-52006) and Skolkovo Foundation for the financial support of this work.

Appendix. Coefficients of expansion of electromagnetic fields in vector spherical harmonics

The coefficients ${}^sA_{mn}^{(0)}$, ${}^sB_{mn}^{(0)}$, ${}^sC_{mn}^{(0)}$ and ${}^sD_{mn}^{(0)}$ appearing in (4) may be represented in the form:

$$\begin{aligned} \begin{Bmatrix} {}^sA_{mn}^{(0)} \\ {}^sB_{mn}^{(0)} \end{Bmatrix} &= ik_0^3 \begin{Bmatrix} {}^sF_{mn}(\mathbf{d}_0) \\ {}^sG_{mn}(\mathbf{d}_0) \end{Bmatrix} + i \begin{Bmatrix} {}^sG_{mn}(-i\mathbf{m}_0) \\ {}^sF_{mn}(-i\mathbf{m}_0) \end{Bmatrix}, \\ \begin{Bmatrix} {}^sC_{mn}^{(0)} \\ {}^sD_{mn}^{(0)} \end{Bmatrix} &= ik_0^3 \begin{Bmatrix} {}^s\tilde{F}_{mn}(\mathbf{d}_0) \\ {}^s\tilde{G}_{mn}(\mathbf{d}_0) \end{Bmatrix} + i \begin{Bmatrix} {}^s\tilde{G}_{mn}(-i\mathbf{m}_0) \\ {}^s\tilde{F}_{mn}(-i\mathbf{m}_0) \end{Bmatrix}, \end{aligned} \quad (\text{A.1})$$

where

$$\begin{aligned} \begin{Bmatrix} {}^sF_{mn}(\mathbf{c}_0) \\ {}^s\tilde{F}_{mn}(\mathbf{c}_0) \end{Bmatrix} &= -\frac{1}{2}(c_{0x} - ic_{0y}) \\ &\times \left[\frac{1}{n} \begin{Bmatrix} {}^sb_{m-1,n-1} \\ {}^s\tilde{b}_{m-1,n-1} \end{Bmatrix} - \frac{1}{n+1} \begin{Bmatrix} {}^sb_{m-1,n+1} \\ {}^s\tilde{b}_{m-1,n+1} \end{Bmatrix} \right] + \frac{1}{2}(c_{0x} + ic_{0y}) \\ &\times \left[\frac{(n-m-1)(n-m)}{n} \begin{Bmatrix} {}^sb_{m+1,n-1} \\ {}^s\tilde{b}_{m+1,n-1} \end{Bmatrix} \right. \\ &\left. - \frac{(n+m+1)(n+m+2)}{n+1} \begin{Bmatrix} {}^sb_{m+1,n+1} \\ {}^s\tilde{b}_{m+1,n+1} \end{Bmatrix} \right] \\ &+ c_{0z} \left[\frac{n-m}{n} \begin{Bmatrix} {}^sb_{m,n-1} \\ {}^s\tilde{b}_{m,n-1} \end{Bmatrix} + \frac{n+m+1}{n+1} \begin{Bmatrix} {}^sb_{m,n+1} \\ {}^s\tilde{b}_{m,n+1} \end{Bmatrix} \right]; \end{aligned} \quad (\text{A.2})$$

$$\begin{aligned} \begin{Bmatrix} {}^sG_{mn}(\mathbf{c}_0) \\ {}^s\tilde{G}_{mn}(\mathbf{c}_0) \end{Bmatrix} &= \frac{1}{2}(c_{0y} + ic_{0x}) \frac{(2n+1)}{n(n+1)} \begin{Bmatrix} {}^sb_{m-1,n} \\ {}^s\tilde{b}_{m-1,n} \end{Bmatrix} \\ &- \frac{1}{2}(c_{0y} - ic_{0x}) \frac{(n-m)(n+m+1)(2n+1)}{n(n+1)} \begin{Bmatrix} {}^sb_{m+1,n} \\ {}^s\tilde{b}_{m+1,n} \end{Bmatrix} \\ &+ ic_{0z} \frac{m(2n+1)}{n(n+1)} \begin{Bmatrix} {}^sb_{mn} \\ {}^s\tilde{b}_{mn} \end{Bmatrix}; \end{aligned} \quad (\text{A.3})$$

$$\begin{aligned} \begin{Bmatrix} {}^sb_{mn} \\ {}^s\tilde{b}_{mn} \end{Bmatrix} &= \frac{(n-m)!}{(n+m)!} \frac{1}{k_0^s r_0} \begin{Bmatrix} \zeta_n(k_0^s r_0) \\ \psi_n(k_0^s r_0) \end{Bmatrix} \\ &\times P_n^m(\cos \theta_0) \exp(-im \varphi_0); \end{aligned} \quad (\text{A.4})$$

${}^s r_0$, ${}^s \theta_0$ and ${}^s \varphi_0$ are the spherical coordinates of the position of a chiral molecule in the s th local coordinate system; $\zeta_n(k_0^s r_0) = (\pi k_0^s r_0 / 2)^{1/2} H_{n+1/2}^{(1)}(k_0^s r_0)$ and $\psi_n(k_0^s r_0) = (\pi k_0^s r_0 / 2)^{1/2} J_{n+1/2}(k_0^s r_0)$ are the Riccati–Bessel functions; $H_{n+1/2}^{(1)}(k_0^s r)$ and $J_{n+1/2}(k_0^s r)$ are the Hankel function of the first kind and the Bessel function, respectively [49]; and $P_n^m(\cos \theta_0)$ is the associated Legendre function [49].

In the special case of a chiral molecule located on the common Cartesian axis z (i.e., for ${}^s \theta_0 = 0$ или ${}^s \theta_0 = \pi$), one can obtain simple expressions:

$$\begin{aligned} \begin{Bmatrix} {}^sF_{mn}(\mathbf{c}_0) \\ {}^s\tilde{F}_{mn}(\mathbf{c}_0) \end{Bmatrix} &= -\frac{1}{2} [\delta_{m1}(c_{0x} - ic_{0y}) \\ &- \delta_{m,-1}(c_{0x} + ic_{0y}) n(n+1)] \frac{2n+1}{n(n+1)} \times \\ &\times \frac{1}{k_0^s r_0} \begin{Bmatrix} \zeta'_n(k_0^s r_0) \\ \psi'_n(k_0^s r_0) \end{Bmatrix} P_{n+1}(\cos \theta_0) \\ &+ \delta_{m0} c_{0z} \frac{2n+1}{(k_0^s r_0)^2} \begin{Bmatrix} \zeta_n(k_0^s r_0) \\ \psi_n(k_0^s r_0) \end{Bmatrix} P_{n+1}(\cos \theta_0), \end{aligned} \quad (\text{A.5})$$

$$\begin{aligned} \begin{Bmatrix} {}^sG_{mn}(\mathbf{c}_0) \\ {}^s\tilde{G}_{mn}(\mathbf{c}_0) \end{Bmatrix} &= \frac{1}{2} [\delta_{m1}(c_{0y} + ic_{0x}) \\ &- \delta_{m,-1}(c_{0y} - ic_{0x}) n(n+1)] \frac{(2n+1)}{n(n+1)} \\ &\times \frac{1}{k_0^s r_0} \begin{Bmatrix} \zeta_n(k_0^s r_0) \\ \psi_n(k_0^s r_0) \end{Bmatrix} P_n(\cos \theta_0), \end{aligned} \quad (\text{A.6})$$

where the prime at the function denotes the derivative with respect to its argument; and δ_{mp} is the Kronecker delta equal to unity at $m = p$ and to zero in other cases.

To use the boundary conditions in the problem of a cluster of two spherical particles, one should apply the theorem of addition of vector spherical harmonics [29–31, 42], with which in this case can be, for example, written the expression

$$\begin{aligned} \begin{Bmatrix} {}^2N\xi_{mq} \\ {}^2M\xi_{mq} \end{Bmatrix} &= \\ &= \begin{cases} \sum_{n=|m|}^{\infty} \left[V_{mnq} \begin{Bmatrix} {}^1N\psi_{mn}^{(0)} \\ {}^1M\psi_{mn}^{(0)} \end{Bmatrix} + W_{mnq} \begin{Bmatrix} {}^1M\psi_{mn}^{(0)} \\ {}^1N\psi_{mn}^{(0)} \end{Bmatrix} \right], & |r| < l, \\ \sum_{n=|m|}^{\infty} \left[\tilde{V}_{mnq} \begin{Bmatrix} {}^1N\xi_{mn} \\ {}^1M\xi_{mn} \end{Bmatrix} + \tilde{W}_{mnq} \begin{Bmatrix} {}^1M\xi_{mn} \\ {}^1N\xi_{mn} \end{Bmatrix} \right], & |r| > l, \end{cases} \end{aligned} \quad (\text{A.7})$$

where the lower limit of summation must be assumed equal to 1 for $m = 0$ and to $|m|$ for $m \neq 0$; and l is the distance between the origins of the local coordinate systems (Fig. 1). The functions appearing in (A.7) are defined as follows:

$$\begin{aligned} \begin{Bmatrix} V_{mnq} \\ \tilde{V}_{mnq} \end{Bmatrix} &= \begin{Bmatrix} U_{mnq} \\ \tilde{U}_{mnq} \end{Bmatrix} - k_0 l \begin{Bmatrix} n-m \\ n(2n-1) \end{Bmatrix} \begin{Bmatrix} U_{m,n-1,q} \\ \tilde{U}_{m,n-1,q} \end{Bmatrix} \\ &+ \frac{n+m+1}{(n+1)(2n+3)} \begin{Bmatrix} U_{m,n+1,q} \\ \tilde{U}_{m,n+1,q} \end{Bmatrix}, \end{aligned}$$

$$\left\{ \begin{array}{l} W_{mnq} \\ \tilde{W}_{mnq} \end{array} \right\} = -\frac{imk_0 l}{n(n+1)} \left\{ \begin{array}{l} U_{mnq} \\ \tilde{U}_{mnq} \end{array} \right\}, \quad (\text{A.8})$$

$$\left\{ \begin{array}{l} U_{mnq} \\ \tilde{U}_{mnq} \end{array} \right\} = \left[\frac{(n-m)!(q+m)!}{(n+m)!(q-m)!} \right]^{1/2} \times \sum_{\sigma=|n-q|}^{n+q} \frac{i^{n-q-\sigma}}{k_0 l} \left\{ \begin{array}{l} (-1)^m (2n+1) \zeta_{\sigma}(k_0 l) C_{qmm, -m}^{\sigma 0} C_{q0n0}^{\sigma 0} \\ (2\sigma+1) \psi_{\sigma}(k_0 l) C_{qmn0}^{nm} C_{q0\sigma 0}^{n0} \end{array} \right\}, \quad (\text{A.9})$$

where $C_{\alpha\beta\gamma}^{cy}$ are the Clebsch–Gordan coefficients [50].

References

- Lindell I.V., Sihvola A.H., Tretyakov S.A., Viitanen A.J. *Electromagnetic Waves in Chiral and Bi-isotropic Media* (Boston: Artech House Publishers, 1994).
- Wang B., Zhou J., Koschny T., Soukoulis C.M. *Appl. Phys. Lett.*, **94**, 151112 (2009).
- Zhou J., Dong J., Wang B., Koschny Th., Kafesaki M., Soukoulis C.M. *Phys. Rev. B*, **79**, 121104(R) (2009).
- Plum E., Zhou J., Dong J., Fedotov V.A., Koschny T., Soukoulis C.M., Zheludev N.I. *Phys. Rev. B*, **79**, 035407 (2009).
- Gansel J.K., Thiel M., Rill M.S., Decker M., Bade K., Saile V., von Freymann G., Linden S., Wegener M. *Science*, **325**, 1513 (2009).
- Chew H. *J. Chem. Phys.*, **87**, 1355 (1987).
- Chew H. *Phys. Rev. A*, **38**, 34s10 (1988).
- Klimov V.V., Letokhov V.S. *Laser Phys.*, **15**, 61 (2005).
- Klimov V.V. *Opt. Commun.*, **211**, 183 (2002).
- Blanco L.A., Garcia de Abajo F.J. *Phys. Rev. B*, **69**, 205414 (2004).
- Klimov V.V., Guzатов D.V. *Phys. Rev. B*, **75**, 024303 (2007).
- Liaw J.-W., Chen C.-S., Chen J.-H. *J. Quant. Spectrosc. Radiat. Transfer*, **111**, 454 (2010).
- Klimov V.V., Guzатов D.V., Ducloy M. *Europhys. Lett.*, **97**, 47004 (2012).
- Guzатов D.V., Klimov V.V. *New J. Phys.*, **14**, 123009 (2012).
- Klimov V.V., Guzатов D.V. *Usp. Fiz. Nauk*, **182**, 1130 (2012).
- Golubkov A.A., Makarov V.A. *Usp. Fiz. Nauk*, **165**, 339 (1995) [*Phys. Usp.*, **38**, 325 (1995)].
- Golubkov A.A., Makarov V.A. *Izv. RAN, Ser. Fiz.*, **59** (12), 93 (1995).
- Drude P. *Lehrbuch der Optik* (Leipzig: Verlag von S.Hirzel, 1906).
- Born M. *Optika: uchebnik elektromagnitnoi teorii sveta* (Optics: A Textbook on the Electromagnetic Theory of Light) (Kharkov–Kiev: GNTI Ukrainy, 1937).
- Bokut B.V., Serdyukov A.N., Fedorov F.I. *Kristallografiya*, **15**, 1002 (1970) [*Sov. Phys. Crystallogr.*, **15**, 871 (1971)].
- Horsley S.A.R. *Phys. Rev. A*, **84**, 063822 (2011).
- Agranovich V.M., Ginzburg V.L. *Crystal Optics with Spatial Dispersion and Excitons* (Berlin: Springer-Verlag, 1984; Moscow: Nauka, 1965).
- Quinten M., Kreibig U. *Appl. Opt.*, **32**, 6173 (1993).
- Borghese F., Denti P., Toscano G., Sindoni O.I. *Appl. Opt.*, **18**, 116 (1979).
- Bruning J.H., Lo Y.T. *IEEE Trans. Antennas Propag.*, **19**, 378 (1971).
- Fuller K.A., Kattawar G.W. *Opt. Lett.*, **13**, 90 (1988).
- Hamid A.K. *J. Electromagn. Waves Appl.*, **10**, 723 (1996).
- Mackowski D.W. *J. Opt. Soc. Am. A*, **11**, 2851 (1994).
- Fuller K.A. *J. Opt. Soc. Am. A*, **11**, 3251 (1994).
- Dufva T.J., Sarvas J., Sten J.C.-E. *Progr. Electromag. Res.*, **4**, 79 (2008).
- Gerardy J.M., Ausloos M. *Phys. Rev. B*, **25**, 4204 (1982).
- Waterman P.C. *Phys. Rev. D*, **3**, 825 (1971).
- Mishchenko M.I., Travis L.D. *Opt. Commun.*, **109**, 16 (1994).
- Mishchenko M.I., Mackowski D.W., Travis L.D. *Appl. Opt.*, **34**, 4589 (1995).
- Mishchenko M.I., Travis L.D., Mackowski D.W. *J. Quant. Spectrosc. Radiat. Transfer*, **55**, 535 (1996).
- Mackowski D.W., Mishchenko M.I. *J. Opt. Soc. Am. A*, **13**, 2266 (1996).
- Mackowski D.W. *J. Quant. Spectrosc. Radiat. Transfer*, **70**, 441 (2001).
- Mishchenko M.I., Travis L.D., Laci A.A. *Scattering, Absorption, and Emission of Light by Small Particles* (New York, Goddard Institute for Space Studies, 2004).
- Chew H., McNulty P.J., Kerker M. *Phys. Rev. A*, **13**, 396 (1976); Erratum: *Phys. Rev. A*, **14**, 2379 (1976).
- Bohren C.F. *Chem. Phys. Lett.*, **29**, 458 (1974).
- Stratton J.A. *Electromagnetic Theory* (New York: McGraw Hill, 1941; Moscow – Leningrad.: Gostehizdat, 1948).
- Ivanov E.A. *Difraktsiya elektromagnitnykh voln na dvukh telakh* (Diffraction of Electromagnetic Waves on Two Bodies) (Minsk: Nauka i tekhnika, 1968).
- Klimov V.V., Ducloy M. *Phys. Rev. A*, **69**, 013812 (2004).
- Busse G., Reinert J., Jacob A.F. *IEEE Trans. Microw. Theory Tech.*, **47**, 297 (1999).
- Gomez A., Lakhtakia A., Margineda J., Molina-Cuberos G.J., Nunez M.J., Saiz Ipina J.A., Vegas A., Solano M.A. *IEEE Trans. Microw. Theory Tech.*, **56**, 2815 (2008).
- Gansel J.K., Thiel M., Rill M.S., Decker M., Bade K., Saile V., von Freymann G., Linden S., Wegener M. *Science*, **325**, 1513 (2009).
- Smith D.R., Padilla W.J., Vier D.C., Nemat-Nasser S.C., Schultz S. *Phys. Rev. Lett.*, **84**, 4184 (2000).
- Pendry J.B., Holden A.J., Robbins D.J., Stewart W.J. *IEEE Trans. Microw. Theory Tech.*, **47**, 2075 (1999).
- Abramowitz M., Stegun I.A. (Eds) *Handbook of Mathematical Functions with Formulas, Graphs, and Mathematical Tables* (New York: Dover, 1972; Moscow: Nauka, 1979).
- Varshalovich D.A., Moskalev A.N., Khersonskii V.K. *Quantum Theory of Angular Momentum* (Singapore: World Scientific, 1988; Leningrad: Nauka, 1975).